Carbohydrate Polymers 84 (2011) 887–893

Contents lists available at ScienceDirect

Carbohydrate Polymers

journal homepage: www.elsevier.com/locate/carbpol

A novel chitosan/polyoxometalate nano-complex for anti-cancer applications

Deepthy Menon[a,*], Reny Thankam Thomas[a], Sreeja Narayanan[a], S. Maya[a], R. Jayakumar[a], Firasat Hussain[b,c], Vinoth-Kumar Lakshmanan[a], S.V. Nair[a]

[a] Amrita Centre for Nanosciences & Molecular Medicine, Amrita Institute of Medical Sciences and Research Centre, Amrita Vishwa Vidyapeetham, Kochi 682041, Kerala, India
[b] Institute of Inorganic Chemistry, University of Zurich, Winterthurerstrass 190, CH-8057 Zurich, Switzerland
[c] Department of Chemistry, Nanoscience and Nanotechnology, University of Delhi, Delhi 110007, India

ARTICLE INFO

Article history:
Received 4 November 2010
Received in revised form 7 December 2010
Accepted 8 December 2010
Available online 15 December 2010

Keywords:
Chitosan
Polyoxometalate
Ionotropic gelation
Nanocomplex
Anticancer
Flowcytometry

ABSTRACT

Polyoxometalates (POMs) show great molecular diversity and have significant applications in material science as well as in medicine. In this study, nano-complexation of a novel europium containing polyanion $[Cs\subset Eu_6As_6W_{63}O_{218}(H_2O)_{14}(OH)_4]^{25-}$ (EuWAs) with biocompatible chitosan was achieved through ionotropic gelation technique without the aid of any cross-linker. Thus obtained chitosan/EuWAs nanocomplex was characterized using DLS and Zeta analysis, FT-IR, SEM, AFM, TG/DTA, EDAX and fluorescence spectroscopy. The cross-linking efficiency of EuWAs with chitosan was calculated to be 81% and the release profile recorded at physiological pH was slow and sustained. Cytotoxicity assays performed on a host of cancer cell lines, viz., KB, MCF-7, PC-3 and A549 proved the anticancer activity of the nanocomplex and flow cytometry studies revealed that reactive oxygen species generation can be the plausible mechanism for the apoptosis induced by this material. Our study has thus indicated the feasibility of using chitosan/EuWAs nano-complex for anticancer applications.

1. Introduction

Natural and synthetic biodegradable polymers as nanocarriers find immense applications in nanomedicine as controlled release vehicles for various drugs, peptides, proteins, etc. in both targeted and non-targeted forms (Duncan, 2006). The pharmacokinetics and dynamics of the nanomedicine is significantly influenced by the choice of the carrier material (Park, Saravanakumar, Kim, & Chan Kwon, 2010). Amongst the various natural polymers suggested for nanodrug delivery applications, the polysaccharide chitosan has been one of the most extensively studied materials thus far (Janes, Fresneau, Marazuela, Fabra, & Alonso, 2001; Jayakumar, Menon, Manzoor, Nair, & Tamura, 2010). Chitosan is a copolymer of glucosamine and *N*-acetyl glucosamine linked by β 1-4 glucosidic bonds obtained by *N*-deacetylation of chitin, a structural polysaccharide found in the shells of crabs and the exoskeleton of shrimps (Kumar, Muzzarelli, Muzzarelli, Sashiwa, & Domb, 2004). Chitosan has free amine as well as hydroxyl groups, and can be modified to obtain different chitosan derivatives (Anitha et al., 2009; Jayakumar, Nwe, Tokura, & Tamura, 2007; Jayakumar, Prabaharan, et al., 2010; Jayakumar, Prabaharan, Reis, & Mano, 2005), rendering them with chelating or bioadhesive properties (Lee, Park, & Robinson, 2000).

Polyoxometalates (POMs) are a class of stable metal-oxide clusters ideally suited for biological applications owing to their promising antiviral and antitumoral properties as well as their use as HIV inhibitors, antibiotics, luminescent and magnetic materials, etc. (Rhule, Hill, & Judd, 1998; Kortza et al., 2009). In the studies on the therapeutic effects of POMs against cancer and leukemia, it was proved that the anti-tumor activity of $[Mo_7O_{24}]^{6-}$ is even better than that of certain commercially available drugs such as cisplatin (Wang et al., 2000, 2003). These properties can be attributed to their molecular and electronic structural versatility and reactivity (Casan-Pastor & Gomez-Romero, 2004). The primary reason that deters the applicability of POMs in medicine is their instability in water at physiological pH resulting in their degradation into a mixture of inorganic products. Furthermore, the cellular toxicity induced by POMs can also hinder their medical use. An improvement in their physiological stability as well as biological activity can be achieved by appropriate modifications of their surface charge, polarity, redox potential, etc., by combining POMs with nano drug delivery carriers based on biodegradable polymers. Zhai et al. have reported the use of a water-in-oil emulsion technique to prepare $Si_2W_{18}Ti_6$ polyoxometalate loaded starch nanoparticles with enhanced antitumor effects (Zhai, Li, Zhang, Wang, & Li, 2008).

The objective of the present study is to evaluate the potential of a novel europium containing polytungstoarsenate (III) polyanion ($[Cs\subset Eu_6As_6W_{63}O_{218}(H_2O)_{14}(OH)_4]^{25-}$) complexed with the biopolymer chitosan, as a cancer nanomedicine. Chitosan–EuWAs nanocomplexes were synthesized by ionotropic gelation technique.

* Corresponding author. Tel.: +91 484 2801234; fax: +91 484 2802020.
E-mail addresses: deepthymenon@aims.amrita.edu, deepsmenon@gmail.com (D. Menon).

0144-8617/$ – see front matter © 2010 Elsevier Ltd. All rights reserved.
doi:10.1016/j.carbpol.2010.12.030

Further the nanocomplex was structurally characterized and its release profile was evaluated spectrofluorimetrically. The antitumor activity of the nanocomplex was investigated on a host of cancer cell lines in comparison to bare EuWAs and a possible mechanism of antitumor action was also explored.

2. Experiments

2.1. Materials

Chitosan (low molecular weight with a degree of deacetylation of 75–85%) and Lysozyme were purchased from Sigma–Aldrich, USA. Acetic acid was purchased from Qualigens India Pvt. Ltd.

2.2. Preparation of chitosan/EuWAs nanocomplexes

Polytungstoarsenate(III) polyanion ($[Cs\subset Eu_6As_6W_{63}O_{218}(H_2O)_{14}(OH)_4]^{25-}$) [hereafter abbreviated as EuWAs] was obtained from Dr. Firasat Hussain, University of Zurich, which was prepared according to the reported method (Hussain et al., 2009). To prepare the nanocomplex of EuWAs with chitosan, the polymer was dissolved in 1% acetic acid and the polyoxometalate was dissolved in minimum volume (typically 500 μl) of MilliQ water. EuWAs solution was added into the chitosan solution drop-wise under controlled sonication conditions for 2 min, yielding a stable colloidal suspension. Chitosan–EuWAs nanocomplex was separated by centrifugation for 45 min at 20,000 rpm (HERMLE Z36HK, Germany). Various experiments were carried out by altering the polymer-to-drug ratio as well as other preparation conditions and the optimal parameters that yielded the stable colloid were noted.

2.3. Physico-chemical characterization of chitosan/EuWAs nanocomplexes

Particle size as well as the morphology of the nanocomplex was analyzed by atomic force microscopy (AFM) [Model JEOL JSPM-5200] and scanning electron microscopy (SEM) [Model JEOL JSM-6490LA]. The hydrodynamic diameter and its distribution were measured by the laser light scattering technique using a particle size analyzer (Nicomp Particle Size Analyzer 38/ZLS, USA). Fourier transform infrared (FTIR) spectroscopy was used to identify the infrared absorption peaks, with the spectral scan set for the frequency range spanning from 4000 to 400 cm^{-1} using a Perkin Elmer Spectrum RX-1. Material composition was analyzed by Energy Dispersive X-Ray (EDX) spectroscopy (JEOL JSM-6490LA). Thermal stability of the nanocomplex was analyzed using thermogravimetric technique (SII TG/DTA 6200 EXSTAR) by heating the samples to 550 °C at a rate of 10 °C/min in nitrogen atmosphere. Fluorescence emission from EuWAs as well as the nanocomplex was measured using a spectrofluorimeter (HORIBA, JOBIN YVON Fluoromax 4) in the wavelength range 200–900 nm.

2.4. Entrapment and loading studies using spectrofluorimetry

The entrapment efficiency of EuWAs within the nanocomplex was determined using fluorescence spectroscopy. Initially a standard curve of varying concentrations of bare EuWAs was plotted by recording the characteristic fluorescence emission from Europium (Eu) at 612 nm for an excitation wavelength of 393 nm. The loading efficiency of EuWAs in chitosan matrix was determined by quantifying the entrapped EuWAs. Briefly, the nanocomplex was centrifuged at 20,000 rpm for 30 min and the supernatant was analyzed using fluorescence spectroscopy to determine the amount of un-entrapped EuWAs in the formulation. The previously prepared standard curve was used to determine the concentration of free EuWAs in the supernatant. Loading and entrapment efficiencies were determined by the following formulae:

$$\text{Loading efficiency } (\%) = \frac{M_{np}}{M_{recovered}} \times 100;$$

M_{np} is the mass of EuWAs in nanoparticles and $M_{recovered}$ is the nanoparticles recovered after formulation (yield).

$$\text{Entrapment efficiency } (\%) = \frac{M_{np}}{M_{formulation}} \times 100;$$

M_{np} is the mass of EuWAs in the nanoparticles and $M_{formulation}$ is the mass of EuWAs used in the formulation.

2.5. In vitro release of POMs from chitosan matrix

The *in vitro* release of EuWAs from the nanocomplex was performed at 37 °C in phosphate buffered saline (PBS, pH 7.4) containing 1.6 μg/ml of lysozyme. The nanoformulation was centrifuged at 20,000 rpm for 30 min and the pellet was redispersed in PBS under magnetic stirring. At predetermined time intervals, the samples were centrifuged at 12,000 rpm for 15 min and the supernatant was analyzed spectrofluorimetrically, after which the sample was replaced back into the solution. The standard curve for EuWAs was used to determine its time dependent release profile.

2.6. Cell culture

The cell lines used in the present study were MCF-7 (breast cancer cells), KB (nasopharengeal epidermoid carcinoma), PC-3 (prostate cancer cells) and A549 (lung cancer cells) were procured from National Centre for Cell Sciences, Pune, India. The cell lines were cultivated in Modified Eagle's Medium (MEM, Sigma) supplemented with 10% fetal bovine serum (GIBCO) and 1% penicillin-streptomycin (GIBCO) at 37 °C in humidified environment of 5% CO_2 in an incubator. The medium was replenished every other day and the cells were sub-cultured after attaining 80% confluency. [3-(4, 5-dimethylthiazol-2-yl)-2, 5-diphenyltetrazolium bromide (MTT) and Lactate dehydrogenase (LDH) assay kit were purchased from Sigma–Aldrich, India. Intracellular ROS assessment kit was purchased from Invitrogen, USA.

2.7. Cytotoxicity studies

2.7.1. MTT assay

Cytotoxicity of the chitosan/EuWAs nanocomplex was analyzed using the MTT assay. MTT [3-(4,5-dimethylthiazol-2-yl)-2,5-diphenyltetrazolium bromide] assay is a colorimetric assay based on the selective ability of viable cells to reduce the tetrazolium component of MTT in to purple colored formazan crystals (Liu, Peterson, Kimura, & Schubert, 1997). The cells were harvested at the log phase and were seeded into a 96 well plate at a seeding density of 10^4 cells/ml. After incubating the cell at their log phase with various concentrations of chitosan/EuWAs and bare EuWAs (0.005–1 mg/ml at specific intervals, in triplicates) for 24 h, 10 μl of MTT dye (5 mg/ml) was added into each well. The percentage of cell viability was determined by recording the optical absorbance at 570 nm using a microplate reader (Microtek Power Wave XS US) relative to the non-treated cells. Cell viability was calculated using the following equation:

$$\text{Cell viability } (\%) = \frac{I_{nts}}{Int_{control}} \times 100;$$

Int_s is the OD value of the cells incubated with the nanocomplex and $Int_{control}$ is the OD value of the cells incubated with the culture medium alone.

2.7.2. LDH assay

Lactate dehydrogenase (LDH) is a stable cytoplasmic enzyme which gets released into the culture supernatant upon plasma membrane damage (Mitchell, Santone, & Acosta, 1980). LDH assay was carried out on KB cells by recording the optical absorbance at 500 nm according to reported protocols. KB cells at a density of 10^4/well were seeded into a 96 well plate and incubated for 24 h, following which samples at similar concentration range as that used for MTT, resuspended in medium containing 10% FBS was added to the cells, with untreated cells as low control and 1% Triton X-100 as high control. Cells were then incubated with the samples for 24 h and after centrifugation, the assay reagent (catalyst: dye in the ratio 1:45) was added to the supernatant and incubated at room temperature for 30 min. Optical absorbance was recorded at 490 nm using a microplate reader (Microtek Power Wave XS, US) relative to the untreated cells and the cell viability was calculated as follows:

$$\text{Cell viability}\ \ (\%) = 100 - \frac{(\text{Ta-Lc})}{(\text{Hc-Lc})} \times 100;$$

Ta, test absorbance; Lc, low control; and Hc, high control.

2.8. Quantification of intracellular ROS

Intracellular accumulation of reactive oxygen species (ROS) was determined with dichlorofluorescein-diacetate (H_2DCF-DA, Invitrogen) following manufacturer's protocols. KB cells were chosen as the representative cancer cell line for the ROS induction study. The cells were seeded into 6-well plates at a density of 2×10^5 cells/well, incubated for 10 h and thereafter treated with the nanocomplex at a concentration of 0.5 mg/ml. After 24 h of incubation, the cells were washed and incubated with 5 mM of H_2DCF-DA (in 100% ethanol) at 37 °C for 30 min. The cells were further analyzed for its ROS generation using flow cytometry (BD-FACS-Aria II), with the fluorescence detected using the excitation and emission filters at 488 nm and 530 ± 15 nm respectively.

3. Results and discussions

3.1. Preparation of chitosan/EuWAs nanocomplexes

Chitosan/EuWAs complexation was intended to study the growth inhibitory effects of nanocomplexed EuWAs on cancer cells in comparison to the bare form of POMs. The nanocomplex was prepared by a simple ionotropic gelation technique taking advantage of the polyanionic nature of EuWAs and the polycationic nature of chitosan. Since the anionic polyoxometalate is capable of forming stable colloids with the cationic polymer chitosan, the use of other cross linking agents such as sodium tripolyphosphate (TPP) was excluded in the present study. The influence of varying experimental conditions (sonication time and amplitude, use of cross-linking agent) as well as the concentrations of polymer and POMs was investigated to obtain the complexes of optimal particle size with maximum entrapment efficiency.

The mechanism of interaction between chitosan and EuWAs is likely to be electrostatic. Oxygen on the surface of POMs has a partial double bond which can easily lead to ionization. It is expected that the terminal/bridging oxygen on the surface of EuWAs interacts with the NH_3^+ protonated groups of chitosan to form intermolecular cross-linking which thereby results in the nanocomplexation.

3.2. Optimization of formulation parameters

The effect of various formulation parameters in controlling the particle size as well as the stability of nanoparticles in suspension is very critical. Hence, we analyzed the variations in formulation parameters such sonication time, amplitude, polymer:drug (P:D) ratio and the use of cross-linking agent (TPP) on the nanoparticle formation.

3.2.1. Chitosan:EuWAs ratio

To evaluate the influence of chitosan:EuWAs (P:D) ratio on particle size as well as entrapment efficiency, two different ratios were considered (5:2 and 5:1) for experimentation. Table 1 depicts the variations in entrapment efficiency and mean particle size (measured using DLS) for varying ratios. It was observed that there was an increase in the entrapment of POMs with increase in its initial concentration, with a slight increase in particle size. A maximum entrapment efficiency of 81% was measured for a chitosan:EuWAs ratio of 5:2.

3.2.2. Sonication conditions

Sonication prevents the agglomeration of the formed colloidal particles thereby yielding a well dispersed suspension. Probe sonication was found to be more efficient in decreasing and controlling the particle size than ultrasonication. However, entrapment efficiencies of the probe sonicated samples were lower, thereby making sonication time very critical. It was also observed that sonication amplitude also affected the entrapment of EuWAs within chitosan. In the present experiment, a lower sonication amplitude of 25% resulted in higher entrapment than an amplitude of 35%. This may be attributed to the higher shear force at higher amplitudes which resulted in the disintegration of the polyanion from the polymer matrix. Hence, the sonication conditions were optimized to yield a smaller particle size with better entrapment efficiency.

3.2.3. Effect of cross-linking agent (TPP)

The synthesis of the chitosan/EuWAs nanocomplex was experimented with and without TPP, to observe its effects on the nanocomplexation. It was observed that TPP could reduce the particle size, however by considerably reducing POMs entrapment. This may be attributed to the electrostatic competition between EuWAs and TPP for the amine groups of chitosan. It was noticed that the entrapment efficiency drastically declined from 52% to 35% with increasing concentration of TPP from 20% (w/w) to 40%. Therefore the use of TPP was excluded in this synthesis route. Upon excluding TPP, the entrapment was enhanced to 65% (Table 1).

3.3. Physico-chemical and thermal characterization of the nanocomplex

The nancomplex formed by simple ionotropic gelation technique with a chitosan/EuWAs ratio of 5:2 under controlled sonication conditions without the use of TPP were further characterized for their physico-chemical properties such as size, stability, morphology, thermal stability, fluorescence as well as the entrapment efficiency and release profile.

The hydrodynamic size of the nanocomplexes formed was analyzed by DLS (Fig. 1A). Dynamic light scattering measurements showed that more than ~85% of the particles had hydrodynamic diameters well within 200 nm (intensity weighted distribution). The zeta potential was evaluated to determine the surface charge as well as the stability of colloidal suspension. The complexes showed a zeta potential of +77 mV which indicated its excellent electrostatic stability and positive surface charge.

Fig. 1 represents the AFM (Fig. 1B) and SEM (Fig. 1C and D) images of chitosan/EuWAs nanocomplex. It is clearly evident from the images that nearly monodispersed nanoparticles with spherical morphology and a typical size range of ~240 nm were obtained by this technique.

Table 1
Influence of chitosan/EuWAs ratio on entrapment efficiency and mean particle diameter.

P:D ratio	Entrapment efficiency (%)	Mean particle diameter (nm) (DLS data)
5.1 EuWAs	65.2 ± 5	150 ± 10.2
5.1 EuWAs + 40% TPP	35.8 ± 4	100 ± 11.4
5:2 EuWAs	81.2 ± 8	200 ± 40

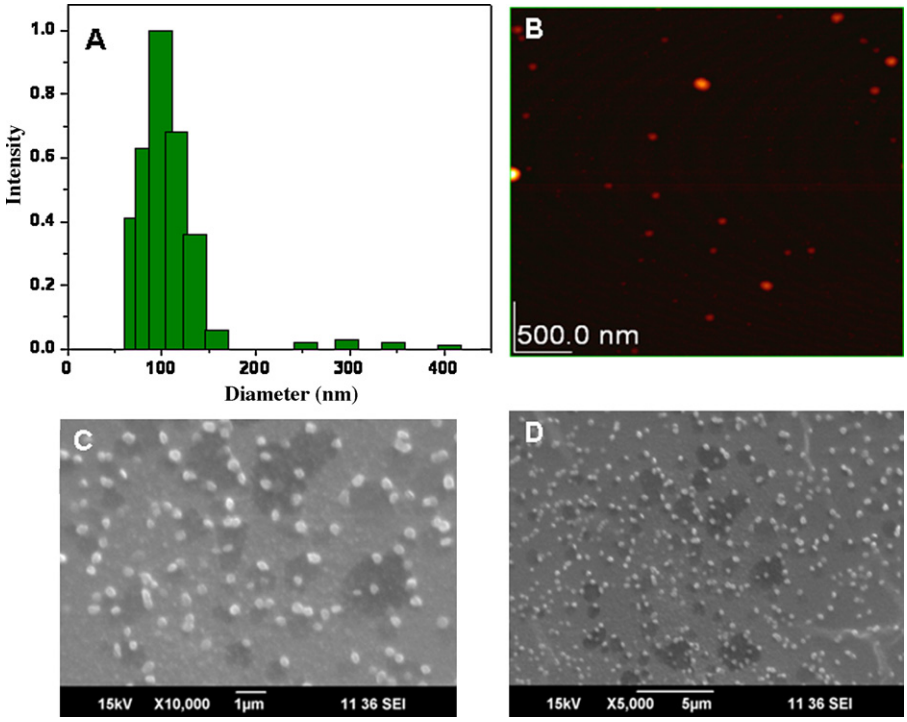

Fig. 1. Size analysis of the EuWAs chitosan nanocomplex; (A) DLS data indicating intensity weighted size distribution of the chitosan/EuWAs nanocomplex; (B) AFM image (C) and (D) SEM images at different magnifications.

In concurrence with the literature reports, FTIR spectrum of EuWAs (blue spectrum) as depicted in Fig. 2 displayed characteristic peaks at 950 (strong – s), 859 (s), 789 (s), 709 (s), 636 (shoulder – sh) and 480 cm^{-1} (medium – m), with the peak at 1636 cm^{-1} corresponding to the molecular water present in the complex (Hussain et al., 2009; Hungerford, Hussain, Patzke, & Green, 2010). Chitosan exhibits peaks between 1650 and 1580 cm^{-1} corresponding to the N–H bending vibration (amines). The peak at 1076 cm^{-1} corresponds to the bridge oxygen (C–O–C) stretching bands (Anitha et al., 2009). FTIR spectrum of the nanocomplex (black spectrum) shown in Fig. 2 revealed the presence of the broad peak between 3400 and 3200 cm^{-1} corresponding to –OH groups and that at 1650–1580 cm^{-1} to the N–H bend of $-NH_2$. The spectra of the nanocomplex exhibited all the characteristic peaks present in EuWAs with slight shifts at 948 (s), 884 (s), 790 (s) and 484 (m), indicative of the complexation. Thus, our FTIR investigations could clearly demonstrate the successful complexation of EuWAs with chitosan.

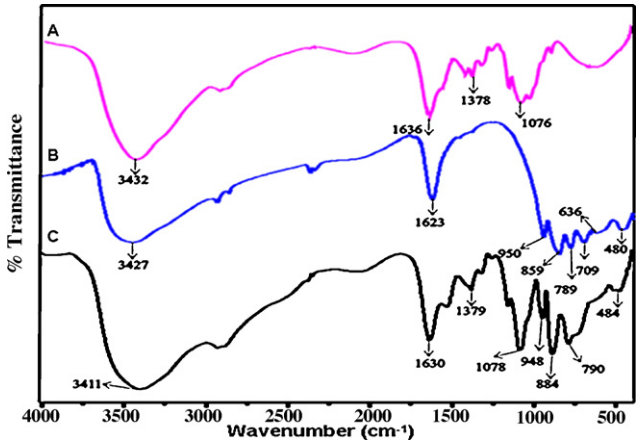

Fig. 2. FTIR spectra of bare (A) chitosan, (B) EuWAs and (C) chitosan/EuWAs nanocomplex.

Elemental analysis carried out using EDAX shown in Fig. 3A revealed the presence of several heavy metals including W, As, Eu, Cs, etc., which helped us to confirm the nanocomplexation of POMs with chitosan matrix.

The presence of Europium in the POMs lattice resulted in a characteristic fluorescence emission peaking at 612 nm for an excitation of 393 nm as evident from Fig. 3B inset. Likewise, the nanocomplex also showed the same characteristic emission due to Eu (Fig. 3B), providing evidence for the incorporation of EuWAs within the chitosan matrix.

Thermogravimetric curves of EuWAs, chitosan and the nanocomplex shown in Fig. 3C revealed that thermal stability of the nanocomplex is enhanced when compared to the bare polymer. This can be attributed to the complexation of chitosan with the thermally stable EuWAs having very less degradation (Hussain et al., 2009). From the thermogram in Fig. 3C, EuWAs showed a slight degradation up to 100 °C which can be attributed to the moisture loss. Further, no degradation was noted up to 500 °C, and ~90% of the sample remained stable without degradation. In the case of chitosan, the degradation up to 100 °C can also be attributed to

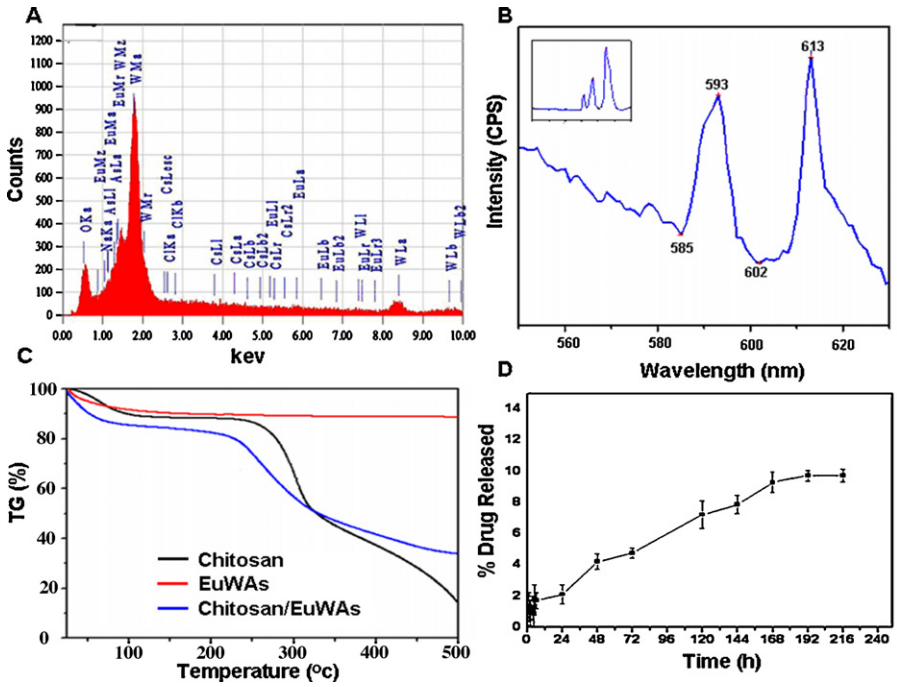

Fig. 3. (A) EDAX analysis of chitosan/EuWAs nanocomplex. (B) Fluorescence emission spectrum of chitosan/EuWAs and bare EuWAs (inset). (C) TGA of EuWAs, chitosan, chitosan/EuWAs nanocomplex. (D) The release profile of EuWAs from the nanocomplex.

the moisture loss and the polymer remains stable till about 228 °C. Subsequently, a steep degradation of the polymeric structure was observed upto ~380 °C. For the nanocomplex, the degradation was observed to start only at 180 °C, with a further slow degradation till 312 °C. The percentage weight remaining at 500 °C for the nanocomplex was more when compared to chitosan. It was also observed that the steepness of the curve is reduced for the nanocomplex indicating its slow degradation in comparison to that of chitosan. In effect, the thermal stability of chitosan is considerably enhanced when complexed with the thermally stable EuWAs.

3.4. Entrapment and release of POMs from the nanocomplex

The loading and entrapment efficiencies of EuWAs within the chitosan matrix were mathematically calculated from the spectrofluorimetric data using the formulae described earlier. The un-entrapped EuWAs remaining in the suspension was quantified by noting the europium fluorescence intensity in the supernatant. From the standard curve, the entrapment efficiency of EuWAs within the nanocomplex was calculated to be 80% and loading efficiency was 64%.

To evaluate the release of EuWAs from the nanocomplex, PBS containing lysozyme at a pH of 7.4, was used as the release medium. The lysozyme concentration used in the present experiment was corresponding to its availability in biological fluids, such as to mimic the *in vivo* system. Lysozyme helps in the enzymatic degradation of the glycosidic bonds in chitosan polymeric chains. This in turn would destabilize the electrostatic interaction between EuWAs and chitosan resulting in its controlled release from the matrix. It was observed that there was a slow, yet steady release of EuWAs over a period of days, with the cumulative release accounting to only about 10% at the end of 9 days (Fig. 3D).

3.5. Anticancer activity studies

3.5.1. Cytotoxicity assay

For MTT assay, a wide range of concentrations of bare EuWAs (5–1000 μg/ml) was tested for its toxicity on different cancer cell lines where a dose dependent cytotoxicity was observed. It was observed that bare material was toxic only at very high concentrations whereas; at concentrations lower than 0.01 mg/ml there was no obvious signs of cell death (Fig. 4A). However, in contrast, chitosan/EuWAs nanocomplex showed significant toxicity to cancer cells even at concentrations as low as 7 μg/ml. This result is a good example for enhanced toxicity caused by nano-encapsulation (Fig. 4B). The IC_{50} value of the nanocomplex was calculated to be ~46 μg/ml, while that of bare EuWAs was ~608 μg/ml, indicating a 13-fold increase in activity on MCF-7. However, on KB cells, the IC_{50} values for the nanocomplex and bare EuWAs were 79 and 522 μg/ml respectively, indicating a 6-fold enhanced activity. Similarly for PC-3 cells, IC_{50} values for the nanocomplex and bare EuWAs were 67 and 613 μg/ml, while for A549 these were respectively 50 and 629 μg/ml, both implying a 9-fold enhancement in activity upon nanoencapsulation. To further confirm the cytotoxicity by lactate dehydrogenase leakage into culture medium (LDH assay), KB cells were chosen as a representative cancer cell line. It was again confirmed that nanoencapsulated EuWAs showed more toxicity to KB cells than bare EuWAs in its native form (Fig. 4C and D). This result correlates well with the MTT observations also and highlights the significance of nanoencapsulation in drug delivery. Additionally an ROS assay was performed to validate the mechanism of cancer cell death due to interaction with the nanocomplex.

3.5.2. ROS quantification

The intracellular reactive oxygen species (ROS) released in cancer cells treated with chitosan/EuWAs was evaluated using flow-cytometry and intracellular ROS chemical sensor, dichlorofluorescin diacetate (H_2DCF–DA). H_2DCF–DA is hydrolyzed by esterases to dichlorofluorescin (DCFH) which is trapped within the cells. This non-fluorescent molecule is oxidized to fluorescent dichlorofluorescein (DCF) by the action of cellular oxidants such as OH^-, $O_2^{\cdot}$, H_2O_2, $^1O_2$. Fig. 5 shows that after 24 h of incubation with the nanocomplex, KB cells exhibit enhanced intracellular ROS release compared to the negative control, which is indicative of an additional stress contributed by the nanocomplex. This signifies

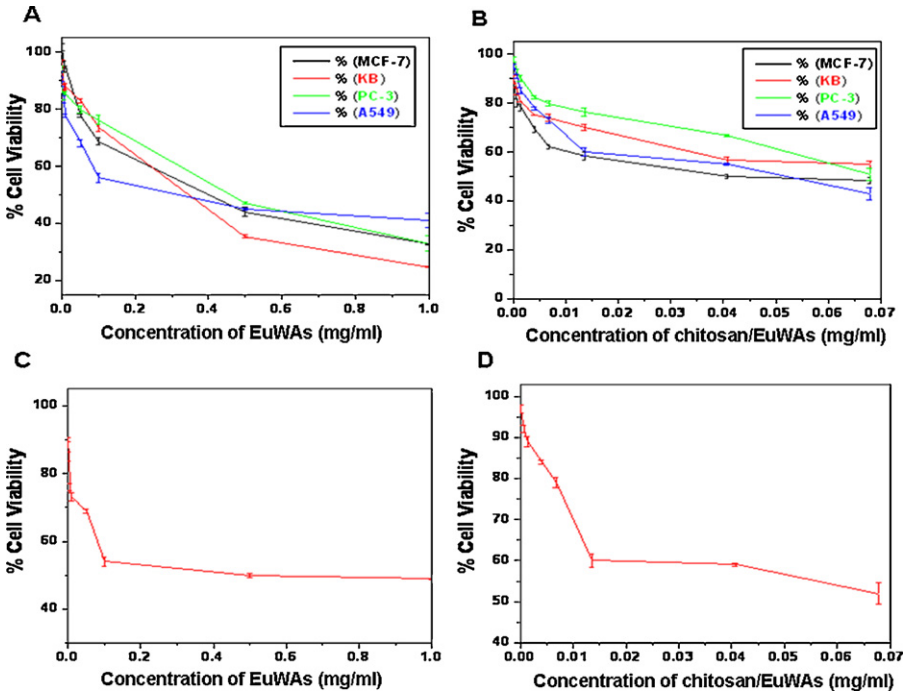

Fig. 4. Cytotoxicity analysis of (A) bare EuWAs and (B) chitosan/EuWAs on MCF-7, KB, PC-3 and A549 cells by 24 h MTT assay. The results show several fold increase in the cytotoxicity caused by nanocomplex at concentrations not observed to be toxic in case of bare and LDH assay results for (C) bare EuWAs and (D) chitosan/EuWAs on KB cells after 24 h incubation.

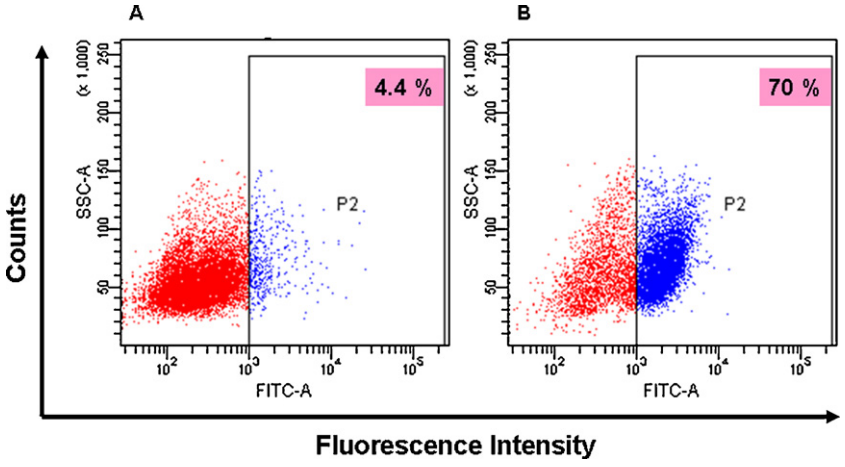

Fig. 5. Measurement of intracellular ROS of KB cells by flow cytometry. Inset shows number of positively labeled cells for DCFH–DA as the percentage of total cell counts in each panel. (A) Untreated negative control cells showing no ROS. (B) Nanocomplex treated sample showing significant levels of ROS.

that EuWAs is capable of generating ROS in the cells, which can be a possible mechanism of cancer cell death.

4. Conclusion

The present study, for the first time in literature, evaluates the potential of chitosan/EuWAs nanocomplex as a cancer nanomedicine. Highly stable monodispersed nanoparticles of size ~200 nm encapsulating EuWAs POMs were prepared by a simple ionotropic gelation method. The nanocomplex showed a slow and sustained drug release profile when tested *in vitro* under physiological conditions. Its anticancer activity was found to be enhanced at doses much lesser as compared to that of bare EuWAs. Generation of intracellular ROS in the nanocomplex treated cancer cells points towards an ROS-mediated stress which causes cancer cell death.

Acknowledgements

The authors R. Jayakumar and Firasat Hussain are grateful to DST, India and EPFL, Switzerland for supporting this project under ISJRP program. The authors acknowledge Dr. Greta R Patzke, Institute of Inorganic Chemistry, University of Zurich, for the collaborative work and valuable suggestions. The authors gratefully acknowledge Department of Science & Technology, Govt. of India for the financial help through Nanoscience & Nanotechnology Initiative monitored by Prof. C.N.R. Rao. The authors are also thankful to Mr. Sajin. P. Ravi, Mr.Girish.C. M. Mr. Sarath, Mr. Sudheesh Kumar P.T and Ms. Sreerekha P. R for their help in SEM, AFM, TG/DTA and FACS studies. We also thank Amrita Vishwa Vidyapeetham for providing all infrastructural support for carrying out the research work.

References

Anitha, A., Divya Rani, V. V., Krishna, R., Sreeja, V., Selvamurugan, N., Nair, S. V., et al. (2009). Synthesis, characterization, cytotoxicity and antibacterial studies of chitosan, *O*-carboxymethyl and *N, O*-carboxymethyl chitosan nanoparticles. *Carbohydrate Polymers*, *78*, 672–677.

Casan-Pastor, N., & Gomez-Romero, P. (2004). Polyoxometalates: From inorganic chemistry to materials science. *Frontiers in Bioscience*, *9*, 1759–1770.

Duncan, R. (2006). Polymer conjugates as anticancer nanomedicines. *Nature Reviews Cancer*, *6*, 688–701.

Hungerford, G., Hussain, F., Patzke, G. R., & Green, M. (2010). The photophysics of europium and terbium polyoxometalates and their interaction with serum albumin: A time-resolved luminescence study. *Physical Chemistry Chemical Physics*, *26*, 7266–7275.

Hussain, F., Spingler, B., Conrad, F., Speldrich, M., Kogerler, P., Boskovic, C., et al. (2009). Caesium-templated lanthanoid-containing polyoxotungstates. *Dalton Transactions*, *23*, 4423–4425.

Janes, K. A., Fresneau, M. P., Marazuela, A., Fabra, A., & Alonso, M. J. (2001). Chitosan nanoparticles as delivery systems for doxorubicin. *Journal of Controlled Release*, *73*, 255–267.

Jayakumar, R., Menon, D., Manzoor, K., Nair, S. V., & Tamura, H. (2010). Biomedical applications of chitin and chitosan based nanomaterials: A short review. *Carbohydrate Polymers*, *62*, 227–232.

Jayakumar, R., Nwe, N., Tokura, S., & Tamura, H. (2007). Sulfated chitin and chitosan as novel biomaterials. *International Journal of Biological Macromolecules*, *40*, 175–181.

Jayakumar, R., Prabaharan, M., Nair, S. V., Tokura, S., Tamura, H., & Selvamurugan, N. (2010). Novel carboxymethyl derivatives of chitin and chitosan materials and their biomedical applications. *Progress in Materials Science*, *55*, 675–709.

Jayakumar, R., Prabaharan, M., Reis, R. L., & Mano, J. F. (2005). Graft copolymerized chitosan-present status and applications. *Carbohydrate Polymers*, *62*, 142–158.

Kortza, U., Müllerb, A., van Slagerenc, J., Schnacke, J., Dalalf, N. S., & Dressel, M. (2009). Polyoxometalates: Fascinating structures, unique magnetic properties. *Coordination Chemistry Reviews*, *253*, 2315–2327.

Kumar, M. N., Muzzarelli, R. A. A., Muzzarelli, C., Sashiwa, H., & Domb, A. J. (2004). Chitosan chemistry and pharmaceutical perspectives. *Chemical Reviews*, *104*, 6017–6084.

Lee, J. W., Park, J. H., & Robinson, J. R. (2000). Bioadhesive-based dosage forms: The next generation. *Journal of Pharmaceutical Sciences*, *89*, 850–866.

Liu, Y., Peterson, D. A., Kimura, H., & Schubert, D. (1997). Mechanism of cellular 3-(4, 5-dimethylthiazol-2-yl)-2, 5-diphenyltetrazolium bromide (MTT) reduction. *Journal of Neurochemistry*, *69*, 581–593.

Mitchell, D. B., Santone, K. S., & Acosta, D. (1980). Evaluation of cytotoxicity in cultured cells by enzyme leakage. *Methods in Cell Science*, *6*, 113–116.

Park, J. H., Saravanakumar, G., Kim, K., & Chan Kwon, I. (2010). Targeted delivery of low molecular drugs using chitosan and its derivative. *Advanced Drug Delivery Reviews*, *62*, 28–41.

Rhule, J. T., Hill, C. L., & Judd, D. A. (1998). Polyoxometalates in Medicine. *Chemical Reviews*, *98*, 327.

Wang, X., Liu, J., Li, J., Yang, Y., Liu, J., Li, B., et al. (2003). Synthesis and antitumor activity of cyclopentadienyltitanium substituted polyoxotungstate $[CoW_{11}O_{39}(CpTi)]^{7-}$ ($Cp{=}\eta^5{-}C_5H_5$). *Journal of Inorganic Biochemistry*, *94*, 279–284.

Wang, X. H., Liu, J. F., Chen, Y. G., Liu, Q., Liu, J. T., & Pope, M. T. (2000). Synthesis, characterization and biological activity of organotitanium substituted heteropolytungstates. *Journal of Chemical Society, Dalton Transactions*, *7*, 1139–1142.

Zhai, F., Li, D., Zhang, C., Wang, X., & Li, R. (2008). Synthesis and characterization of polyoxometalates loaded starch nanocomplex and its antitumoral activity. *European Journal of Medicinal Chemistry*, *43*, 1911–1917.